Network Structure and Methanol Transport Dynamics in Poly(methyl methacrylate)

Adam K. Ekenseair
Dept. of Chemical Engineering, The University of Texas at Austin, Austin, TX 78712

Nicholas A. Peppas
Dept. of Chemical Engineering, and Dept. of Bioengineering, The University of Texas at Austin, Austin, TX 78712

DOI 10.1002/aic.12784
Published online October 27, 2011 in Wiley Online Library (wileyonlinelibrary.com).

The effect of the polymer network structure on methanol transport dynamics in glassy polymers was investigated in both dry and plasticized disks of poly(methyl methacrylate) (PMMA) through gravimetric integral sorption studies. PMMA was synthesized by a controlled free radical polymerization mechanism, crosslinked in bulk with ethylene glycol dimethacrylate, and swollen in methanol under a variety of conditions. In the Case II transport regime, control over the transport rate was shown to depend on the glassy-state properties of the polymer, and the Case II front velocity was found to be proportional to the square root of the crosslinking density. Similarities were observed in the penetrant transport behavior of both dry and plasticized samples at high degrees of crosslinking, and the activation energy of methanol transport at low degrees of crosslinking was found to be similar for both Fickian and Case II mechanisms. © 2011 American Institute of Chemical Engineers *AIChE J,* 58: 1600–1609, 2012

Keywords: anomalous transport, Case II transport, poly(methyl methacrylate), polymer properties, polymerization

Introduction

Deviations from the expected diffusive behavior in regard to the transport of small penetrant molecules, either vapors or liquids, into glassy polymers have been extensively reported. These penetrant–polymer systems exhibit a wide array of dynamic sorption behavior, including simple Fickian transport, Fickian transport with highly concentration-dependent diffusion coefficients, Case II transport, and other anomalous phenomena. The rationale for this diversity in behavior is that in glassy polymers, the relaxation and chain disentanglement process necessary for sample expansion and sorption of penetrants can be a rate-controlling step; thus the transport of the penetrant would proceed at a rate dependent on the mechanical properties of the polymer glass and its thermodynamic compatibility with the penetrant.[1,2] Case II transport, traditionally presented as a limiting case of complete relaxational control over the transport dynamics, has three primary phenomenological traits, all of which are necessary conditions for the occurrence of this mechanism.[3,4]

First, during the penetrant sorption process, there is a sharp front separating a dry polymer core and an outer, penetrant-swollen region. However, the existence of this sharp, inwardly propagating front during integral sorption is not by itself a conclusive indication of Case II behavior. Indeed, sharp penetrant fronts can be observed in most penetrant sorption studies into glassy polymers owing to the strong concentration-dependence of the diffusion coefficient in such cases.[1,5,6]

Second, the sharp front separating dry polymer from fully swollen polymer must advance at a constant rate through the sample until the two fronts (one from each face in a planar integral sorption experiment) meet in the center and sorption ends. In this manner, the initial transport kinetics are forced to scale with time, t, and not $t^{1/2}$ (as is the case in Fickian transport). For this to occur, the penetrant concentration in the swollen region behind the advancing front must maintain a constant concentration throughout the sorption process and constitute an equilibrium, or at least a pseudo-equilibrium, degree of swelling.

Third, there is a Fickian precursor, or foot, that precedes the sharp penetrant front through the polymer. The presence of this precursor was first predicted from theories and later experimentally verified by numerous authors.[7–12] This precursor represents initial Fickian diffusion of the penetrant into the glassy polymer and is responsible for initiating, through solvent-plasticization, the very rapid expansion of the polymer network over the front region.

The presence of this Fickian precursor necessitates another commonly observed trait of Case II transport, namely that there is an induction time associated with sorption in glassy polymers, where the dominance of a particular rate-controlling mechanism has not yet been established. Additionally, integral sorption experiments into glassy polymers are often highly anisotropic in nature due to the stresses imposed by the dry, glassy core on the outer swollen region. Finally, as a further result of these imposed stresses, a material may initially overshoot its final equilibrium penetrant concentration,

Correspondence concerning this article should be addressed to N. A. Peppas at peppas@che.utexas.edu.

as a polymer's ability to hold penetrant can vary with orientation and external stress.

There is currently no way to accurately predict *a priori* the velocity of a Case II penetrant front in an integral sorption experiment from the basic material properties of the polymer and penetrant. The vast majority of investigations has focused on characterizing the qualitative features of Case II transport profiles and attempting to model a transition from Fickian to non-Fickian dynamics, with the result that much is still unknown about how basic material properties affect the transport dynamics within the purely Case II regime. In particular, the effects of the polymer network structure and relaxational behavior have not been sufficiently studied.

A major novel effort of this investigation was a detailed analysis of the effects of crosslinking on the mechanisms of penetrant transport and on the Case II front velocity. The most significant previous finding in terms of how polymer structural parameters affect the transport process has been a determination that the molecular weight of the polymer has no significant effect on the Case II front velocity beyond the critical molecular weight for entanglements.[13] This implies that the number of chain ends and even the related degree of initial free volume have very limited control over the Case II mechanics for identical thermal histories in the presence of stable entanglements. Thus, adding additional points of resistance through chemical crosslinks should have a significant effect on the Case II dynamics.

Previously, Kwei and Zupko[14] noted that increasing the crosslinking density of a polymer while keeping other factors constant resulted in a change from Fickian dynamics at a single lower degree of crosslinking to Case II dynamics at a single higher degree of crosslinking. Additionally, Robert et al.[15] reported that water sorption into spherical microparticles moved from Fickian to anomalous transport dynamics as the crosslinking ratio was increased. Peppas and Urdahl[16] and Smith and Peppas[17] later detailed the effects of crosslinking density on the presence of overshoots in integral sorption experiments; namely that the overshoots were diminished in magnitude and eventually disappeared completely as the degree of crosslinking was increased. The investigation presented in this article sought to add to these previous studies by directly examining first the effects of the crosslinking density on the Case II front velocity. Second, the observation that the transport mechanism can be changed simply by altering the crosslinking density was expounded on.

To study the effects of basic network parameters, including the molecular weight between crosslinks, M_c, and the polymer mesh size, ξ, control over these parameters was necessary. Traditionally, investigators in this field have purchased polymer samples from industrial companies for sorption studies, with the result that little was known or reported on the network structure and other general properties of those polymers. In this investigation, polymer samples were synthesized in house, and the polymer network structure was altered by varying the molar incorporation of crosslinks into the polymer chains. Additionally, a controlled, living free radical polymerization mechanism was utilized to both increase crosslinking efficiency and avoid autoacceleration by controlling the concentration of growing polymer chains.

The most-studied penetrant–polymer system in the literature exhibiting Case II transport is methanol sorption into poly(methyl methacrylate) (PMMA). This system consistently displays Case II transport dynamics at easily accessible experimental conditions and was chosen as the primary system for this investigation. Therefore, samples of PMMA crosslinked during bulk polymerization by the incorporation of difunctional methacrylate comonomers were synthesized. These polymers were then characterized by gel permeation chromatography (GPC), differential scanning calorimetry (DSC), and dynamic mechanical analysis (DMA) to determine basic material properties and verify the polymer network structures produced. Additionally, the effects of temperature were studied, and the behavior was compared with previous investigations.

Materials and Methods

Sample preparation

All reagents were purchased from Sigma–Aldrich (St. Louis, MO) and used as received unless otherwise noted. Homopolymers of methyl methacrylate (MMA) were synthesized using an iniferter-mediated, thermally initiated free radical polymerization. MMA was passed through a prepacked inhibitor removal column (Sigma–Aldrich) to remove hydroquinone before polymerization and was used within 2 weeks of inhibitor removal. The crosslinking agent used was ethylene glycol dimethacrylate (EGDMA). Lauroyl peroxide was added as a thermal initiator in the amount of 0.5 wt % of the total monomer content. Tetraethylthiuram disulfide (TED) was added as an iniferter compound in a 1:1 molar ratio with the thermal initiator.

The components were prepared in a cylindrical glass reaction vessel that was silanized before use with Siliclad™ (Gelest, Morrisville, PA). The mixture was placed in an oxygen-free environment inside a sealed glove box and bubbled with nitrogen for 5 min to remove dissolved oxygen. The vessel was then sealed and placed in a water bath maintained at 60°C and allowed to polymerize for 48 h (~2.3 initiator half-lives). Following synthesis, the polymer cylinders (nominally 25 mm in diameter) were sliced into disks with a nominal thickness of 1 mm by a Isomet™ Low-Speed Saw with diamond wafering blades (Buehler®, Lake Bluff, IL), polished to remove surface defects by an abrasive slurry (Novus #2 Fine Scratch Remover, Savage, MN), and dried and annealed. Unless otherwise noted, samples were dried in a vacuum oven above their T_g until the weight stabilized (generally 4 weeks) and subsequently annealed in a vacuum oven at ~10°C below T_g for 2 weeks. Additionally, the polymers synthesized in this investigation were stored in a standard desiccator loaded with Drierite moisture absorbent (W.A. Hammond Drierite, Xenia, OH) before drying/annealing.

Iniferter chemistry and GPC

An iniferter-mediated mechanism was utilized to control the free radical polymerization of PMMA and circumvent autoacceleration. Iniferter (initiator-chain transfer-termination) compounds typically contain a labile bond, such as a carbamate or disulfide bond, which leads to the formation of stable sulfur radicals.[18] For the case of a carbamate-based molecule or the case of the combination of a disulfide molecule with a traditional free radical initiator, the availability of both carbon and sulfur radicals leads to a reversible capping mechanism and living polymerization scheme, whereby the growing chains are successively terminated via combination with a free sulfur radical and then reinitiated by the cleavage of the newly formed, yet labile, bond.[19–22]

The efficacy of this mechanism stems from the fact that the sulfur radicals formed are relatively less reactive than carbon radicals toward the double bonds found in monomers and thus do not initiate growing polymer chains to a significant extent.[23–25] Additionally, while bimolecular termination of two growing chains can still occur, the cross-termination of a sulfur radical with a carbon radical is preferred even at low conversions when the diffusion resistances are negligible.[26] This preference is only heightened as conversion increases due to increased viscosity and subsequent diffusion limitations, which affect the growing polymer macromolecules to a much greater extent than the small radical sulfur compounds. The low conversion preference has been attributed by some to a higher activation energy for carbon–carbon radical termination vs. carbon–sulfur radical termination.[27] As a result of this behavior, the often problematic phenomenon of autoacceleration can be largely avoided.[27]

One particular concern with the exothermic polymerization of PMMA in bulk was supplying adequate heat transfer, so that autoacceleration as a result of a high core temperature does not occur. This deficiency resulted in significant spatial dependencies of the molecular weights (data not shown). However, the addition of an iniferter compound, like TED, had the ultimate effect of retarding the reaction kinetics, thus preventing temperature-induced autoacceleration and giving homogeneous polymer cylinders. The significant reduction in the overall molecular weight, the number-average molecular weight was reduced from 1,470,000 to 139,000 g/mol, was consistent with the elimination of autoacceleration. In addition to the circumvention of autoacceleration, this polymerization mechanism was chosen for its ease of use in bulk polymerizations, as no solvent was required, its negligible addition of impurities such as heavy metals, and previously demonstrated use in polymerizations of 2-hydroxyehtyl methacrylate and MMA.[28–31]

Polymer characterization

The molecular weights and molecular weight distribution of uncrosslinked polymer samples were determined by a GPC system consisting of a refractometer (Optilab DSP, Wyatt Technology, Santa Barbara, CA) and a multiangle laser light scattering detector (DAWN EOS, Wyatt Technology). The system used a series of two identical polymer labs columns packed with crosslinked polystyrene beads (5 μm bead size, mixed-C pore size). For PMMA, samples of polymer were dissolved in tetrahydrofuran (THF) at a concentration of 5–10 mg/mL, and 60 μL of this solution was injected into the GPC system with THF as the carrier solvent.

The thermal properties of the polymer samples were characterized by DSC (Perkin Elmer DSC 7, Perkin Elmer, Waltham, MA) using a heat/cool/heat method at a heating/cooling rate of 10°C/min. The T_g was determined as the halfway point during the change in heat capacity of the polymer associated with the transition from glass to rubber (1/2 ΔC_p method).

DMA (DMA 983, TA Instruments, New Castle, DE) was used to determine basic mechanical properties. Rectangular samples ($\sim 2 \times 8 \times 20$ mm^3) were cut for each polymer to be tested. Once prepared, the samples were placed into the DMA device, and the device was run on resonant mode with a fixed oscillation amplitude of 0.30 mm from 60 to 180°C at 5°C/min (or higher temperatures as needed). In this manner, the shear storage modulus, G'; the shear loss modulus, G''; the onset T_g based on G'; and the tan δ peak T_g were determined.

Gravimetric studies

Disks of PMMA were suspended in methanol (Certified ACS Grade, Fisher Scientific, Pittsburgh, PA) in a glass jar on a raised aluminum mesh that occluded less than 3% of the lower disk surface. The glass jars were then placed in a constant-temperature water bath. Weight measurements were taken at time intervals by removing a disk from the penetrant, drying the surface, and recording both the weight in air and the weight in a nonsolvent (water) using an Ohaus analytical plus balance (Ohaus, Pine Brook, NJ). For each experiment, sets of three disks were immersed at the same time and all disks were measured at each time point. Additionally, thickness and diameter measurements were taken both before immersion in methanol, and once the disks have reached equilibrium using a digital caliper (Brown and Sharpe, North Kingstown, RI). Finally, disks were taken directly from a vacuum oven after drying/sub-T_g annealing and once the oven had cooled slowly to near room-temperature.

Data analysis

Data analysis of gravimetric integral sorption experiments was accomplished primarily by application of the power-law model:

$$\frac{M_t}{M_\infty} = kt^n \tag{1}$$

where M_t is the mass of penetrant absorbed at a time t, M_∞ is the equilibrium mass of absorbed penetrant, k is a proportionality constant, and n is the power-law exponent.[5] This equation is derived from the short time ($M_t/M_\infty < 0.60$) approximation of the rigorous solution to Fick's second law, where the binary diffusion coefficient is contained within k and $n = 0.5$.[5] In Case II transport, the fractional mass uptake, M_t/M_∞, is directly proportional to time, and thus, n is 1.0. Any behavior that falls between these two extremes is generally assumed to involve a combination or superposition of the two mechanisms and is simply referred to as anomalous behavior with power-law exponent values of $0.5 < n < 1.0$.

Additionally, glassy polymers undergoing integral sorption generally go through an induction time, where the dominance of a particular transport mechanism has not yet begun. In Case II transport, this corresponds with the fact that the relaxational process must be initiated by a Fickian precursor, where slow initial diffusion into the polymer is followed by the establishment of advancing fronts. To account for the presence of induction times in integral sorption studies, Eq. 1 was modified by a time-shift to get:

$$\frac{M_t}{M_\infty} = k(t-\tau)^n \tag{2}$$

where τ is the induction time. Data covering the first 60% of sorption were fit to Eq. 2 through a nonlinear regression and values of k, τ, and n were calculated for all investigations.

Systems exhibiting Fickian or near-Fickian fractional mass uptake, M_t/M_∞, profiles were further analyzed to determine the binary diffusion coefficient, D_{12}, through Eq. 3:

$$D_{12} = \frac{k^2\pi^2}{16} \tag{3}$$

where k was determined from Eq. 2 or a linear regression of the data plotted vs. $t^{1/2}$. In addition, Fickian profiles were

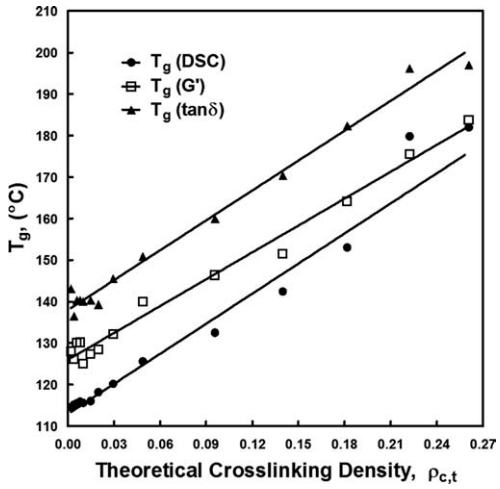

Figure 1. Values of T_g determined for PMMA with varying theoretical crosslinking densities ($\rho_{c,t}$) by DSC and DMA (G' and tan δ).

normalized with respect to sample thickness by dividing time by the square of the initial disk thickness. The rationale for this transformation was that the characteristic diffusion time in Fickian transport varies with both the diffusion coefficient and the diffusion path length.[5] In this way, fractional mass uptake curves for disks with varying thicknesses could be collapsed onto a single curve.

Systems exhibiting Case II transport profiles were analyzed to determine the Case II front velocity by Eq. 4:

$$V_{II} = \left(\frac{dW}{dt}\right)\left(\frac{h_0}{W_0}\right) \tag{4}$$

where V_{II} is the Case II front velocity, W is the weight of the disk, dW/dt is the rate of mass uptake of the swelling disk, h_0 is the initial disk thickness, and W_0 is the initial weight of the disk. This expression is valid for Case II transport in the limit where one-dimensional planar transport into the disk can be assumed. As Case II transport involves a steady-state front propagation into a dry polymer core, the initial thickness, initial polymer mass, and rate of mass uptake are all linked.

Results and Discussion

DSC and DMA

DSC and DMA experiments were performed on the synthesized polymers after drying and annealing to determine both the thermal and the mechanical properties of the samples before use in sorption investigations. For this investigation, a critical parameter was the rate at which the T_g changed with changing network structure. Figure 1 shows the variation of the three calculated values of the glass transition temperature with increasing theoretical crosslinking density, $\rho_{c,t}$ (from 0.002 to 0.261). It should be noted that the crosslinking density used herein is the mol fraction of polymer repeat units that are part of a crosslinkage, as defined by Flory.[32] Additionally, the theoretical value was calculated using available reactivity ratios to predict copolymer compositions based on the reaction feed with an assumed crosslinking efficiency of 100%.[33] Although the absolute value of the T_g differed for each method, increasing the crosslinking density by incorporating more crosslinking moieties affected each method in the same, linear manner. This behavior is generally expected and predicted by the Fox–Loshaek Equation:[34]

$$T_g = T_g^0 + K_c\rho \tag{5}$$

where T_g^0 is the glass transition temperature of the uncrosslinked polymer, ρ is the crosslinking density of the polymer as defined by Fox and Loshaek, and K_c is a polymer-specific constant.[34]

Additionally, values of the shear storage modulus, G', are shown in Figure 2 for PMMA samples with varying theoretical crosslinking densities. As shown, G' increased monotonically after a critical crosslinker composition was reached. This indicated that at and below theoretical crosslinking densities of 0.04, the increase in comonomer concentration was creating crosslink points at a much greater rate than after this critical region. This effect was due to the entrapment of entanglements in the network structure.

Values for the molecular weight between entanglements in uncrosslinked polymer, M_e^0, are given in Ferry[35] as 4700, 10,000, and 4800 g/mol for conventionally synthesized, atactic PMMA. These entanglements act as temporary, physical crosslinks in the rubbery state. However, as chemical crosslinks are added to the network structure, some of these entanglements become entrapped, thereby creating permanent physical crosslinks that add to the effective crosslinking density of the polymer. As the degree of chemical crosslinking continues to increase, eventually all of the entanglements present become locked into place and contribute to polymer properties dependent on the crosslinking density. Thus, shear modulus profiles like the one shown in Figure 2 were expected from theory.[35] Additionally, the latter portion of the curve in Figure 2 was fitted to a linear profile, as shown. The resulting y-intercept returned a value of $M_e^0 = 4690$ g/mol for the polymer samples used in this study. This value was in excellent agreement with values typically reported for PMMA and was utilized in this investigation to determine the experimental crosslinking density, ρ_c.

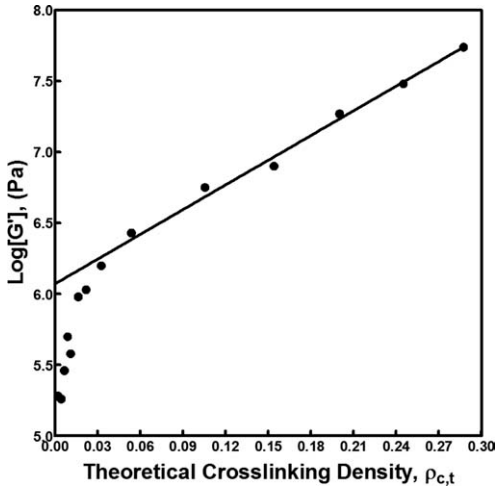

Figure 2. Values of the rubbery plateau shear storage modulus (G') determined by DMA for PMMA crosslinked with EGDMA with varying theoretical crosslinking densities ($\rho_{c,t}$).

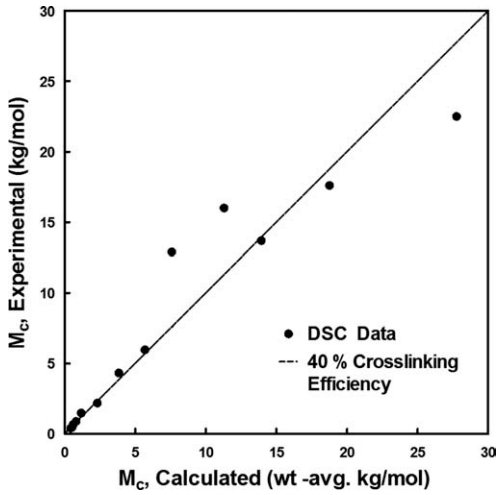

Figure 3. Comparison of molecular weights between crosslinks derived from DSC T_g measurements and weight-averaged reactivity ratio calculations with a crosslinking efficiency of 40% for PMMA crosslinked with EGDMA.

Crosslinking density

DSC measurements of T_g were used to calculate the crosslinking density and M_c through the Fox–Loshaek Equation (Eq. 5) and appropriate data. For PMMA crosslinked with EGDMA in a free-radical polymerization, the Fox–Loshaek constant has been calculated to give:[36]

$$\Delta T_g = (0.78 \times 10^5)\rho \tag{6}$$

Thus, for PMMA crosslinked with EGDMA, the T_g values from Figure 2 were used to calculate ρ and M_c. Figure 3 compares these values of M_c with the weight-averaged theoretical values expected from the reactivity ratios with a crosslinking efficiency of 40% (best fit to the data).

Additionally, DMA analysis was also utilized to determine M_c. Using rubber elasticity theories, the following equation can be derived:[37]

$$\rho_e = \frac{E_1}{6RT} \tag{7}$$

where ρ_e is the total entanglement (chemical and physical) density and E_1 is the bulk storage modulus in the rubbery plateau region, which can be related to the shear storage modulus (G') by:

$$E_1 = G'(1+\mu) \tag{8}$$

where μ is Poisson's ratio, which for PMMA is 0.44.[38] Finally, the effects of chain ends were removed, and ρ_e was related to M_e through Eqs. 9 and 10:

$$\upsilon_e = \rho_e V_0 = \upsilon\left(1 - \frac{M_e}{M_n}\right) \tag{9}$$

$$\upsilon = \frac{\bar{V}}{\bar{v}M_e} \tag{10}$$

where V_0 is the volume of the polymer before expansion, υ is the number of mols of network chain segments including chain ends, $\bar{V}$ is the total volume of the sample, and $\bar{v}$ is the specific volume of the polymer.

Values of M_c were thusly calculated from values of M_e with entanglements subtracted assuming $M_{e,0} = 4690$ g/mol (as determined before). The M_c values were then used to calculate an experimental crosslinking density, ρ_c. The resulting approximate crosslinking efficiency was 38% (data not shown).

Drying and annealing

To remove the unreacted monomer from the PMMA samples, disks were first dried at 10°C below their T_g in a vacuum oven for an extended period of time until the weight stabilized. This resulted in a pseudo-Fickian desorption profile and required 6 months to complete the drying process. The greatest change in polymer disk weight, as well as amount of monomer removed, occurred in the first 2 weeks. Figure 4 shows the effect that varying drying times had on the sorption kinetics of methanol at 30°C. Within the first 24 h, there was an initial loss of ~0.25 wt % of polymer mass, which was attributed to removal of moisture from the PMMA disks. PMMA is somewhat moisture absorptive due to its carbonyl groups and can absorb up to 2 wt % in moisture, though this will be reduced with increased molecular weight and crosslinking.[39] Additionally, the polymers synthesized in this investigation were primarily stored in a standard desiccator loaded with Drierite moisture absorbent, and as such would be expected to retain only a small percentage of water.

The power-law exponent, n, fits for the transport curves at varying drying times are shown in Figure 4. As more MMA was removed from the polymer disks, the behavior began to shift from Fickian ($n = 0.5$) to non-Fickian ($n = 0.71$), or anomalous, transport kinetics. However, due to the sensitive nature of power-law analyses near an n of 0.5, only the 13-day drying time demonstrated a statistically significant change from the other drying times. In addition, the apparent diffusion coefficient, as determined by the kinetic parameter k, decreased, and the induction time necessary to establish the transport profiles increased in statistically significant trends with continued drying up to 7 days drying (13 days

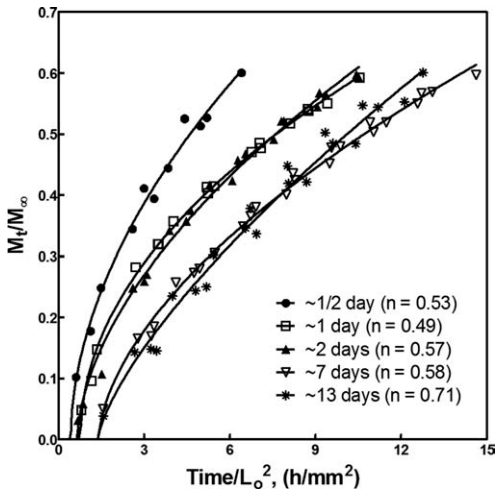

Figure 4. Power-law model analysis on transport kinetics into PMMA disks with a crosslinking density of 0.023, dried at 10°C below T_g for varying times, and swollen in methanol at 30°C.

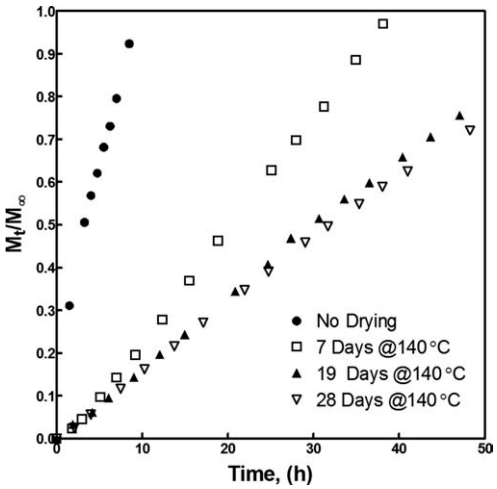

Figure 5. Effect of drying time on PMMA disks with a crosslinking density of 0.023 dried at 10°C above T_g and swollen in methanol at 30°C.

drying yielded non-Fickian transport). After 4 months of drying time, uncrosslinked PMMA displayed purely Case II transport kinetics (data not shown).

Figure 5 shows the effects that super-T_g drying had on the transport kinetics of crosslinked PMMA disks in methanol at 30°C. The Case II front velocity, V_{II}, decreased as drying continued from 7 to 28 days. After 4 weeks, the disks were completely dry, and no change was noticed in the transport dynamics. It can be difficult to discern by Figure 5, but the Fickian mechanism was seen once again with no drying of the polymer disks. Additionally, as cooling below the T_g after drying results in a nonequilibrium state, the polymer disks were annealed for 2 weeks after drying. However, this annealing process was found to have no appreciable effect on the transport mechanism or V_{II} (data not shown).

Effect of temperature

The effects of temperature on the penetrant transport process have been previously studied. However, it was desired to verify that the PMMA samples synthesized in this investigation behave in a comparable manner. Briefly, Thomas and Windle[40] noted several key effects that temperature had on methanol transport into PMMA samples. First, the rate of mass uptake displayed the typical Arrhenius dependence on temperature (Eq. 11), though in this case the Case II front velocity, V_{II}, was the parameter of interest rather than the binary diffusion coefficient:

$$V_{II} = V_{II,0} \exp\left(-\frac{E_a}{RT}\right) \tag{11}$$

where $V_{II,0}$ is the Case II front velocity at 0 K, E_a is the activation energy of Case II penetrant transport, T is the temperature in K, and R is the ideal gas constant ($R = 1.987$ cal/(mol K)).

Second, as the temperature was increased further, deviations from Case II dynamics were observed. Basically, as the Case II front velocity continued to increase, at some point the diffusion of methanol through the swollen layer behind the Case II front could no longer maintain a constant methanol concentration at the front. As a result, the Case II front diminished in magnitude as it propagated through the polymer, and the velocity of the front decreased concomitantly. Additionally, as the temperature of a system is increased, the rate of relaxation of the polymer increases and eventually becomes comparable to the diffusion rate of the penetrant, at which point deviations from Case II transport will also occur. Finally, in the purely Case II regime, Thomas and Windle[40,41] reported an activation energy for transport, E_a, of 25 kcal/mol.

Figure 6 displays the penetrant transport curves for methanol into PMMA from 25 to 35°C. As can be seen from the power-law analysis of the data, all samples displayed Case II transport, except the data at 35°C, which showed a slight deviation from Case II dynamics. Additionally, as the temperature was increased, the front velocity increased and the magnitude of the induction time decreased. The values of V_{II} plotted vs. $1/T$ were fit with a linear regression to the transformed Arrhenius expression (Eq. 12):

$$\ln(V_{II}) = \ln(V_{II,0}) - \left(\frac{E_a}{R}\right)\left(\frac{1}{T}\right) \tag{12}$$

The value of the activation energy thus calculated was 25.5 kcal/mol ($R^2 = 0.996$), which is in excellent agreement with previous research.

An additional consideration that was taken into account was the effect that the equilibrium penetrant volume fraction, φ_s, had on the front velocity. It has been reported that the velocity of the Case II front varies linearly with φ_s with a unit slope.[40] Data collected in this study (not shown) corroborated this relationship. Thus, the value of φ_s should always be taken into account. When the data were then normalized by φ_s, the trend was essentially unchanged, and the recalculated activation energy was 23.8 kcal/mol.

Finally, in an analogous manner, the dependence of the diffusion coefficient on temperature for polymer disks dried/annealed at 10°C below T_g for 24 h was determined by an Arrhenius expression:

$$\ln(D_{12}) = \ln(D_0) - \left(\frac{E_a}{R}\right)\left(\frac{1}{T}\right) \tag{13}$$

where D_{12} is the binary diffusion coefficient, and D_0 is the binary diffusion coefficient at 0 K. In this instance, the polymer disks all displayed Fickian sorption kinetics due to the plasticizing effect of the 2.0–2.5 wt % of unreacted monomer

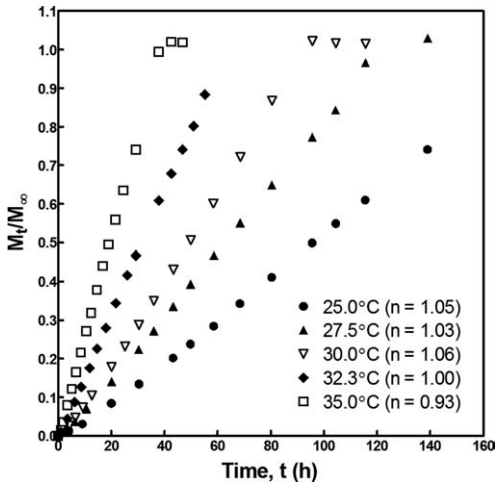

Figure 6. Effect of temperature on PMMA disks with a crosslinking density of 0.023 and swollen in methanol.

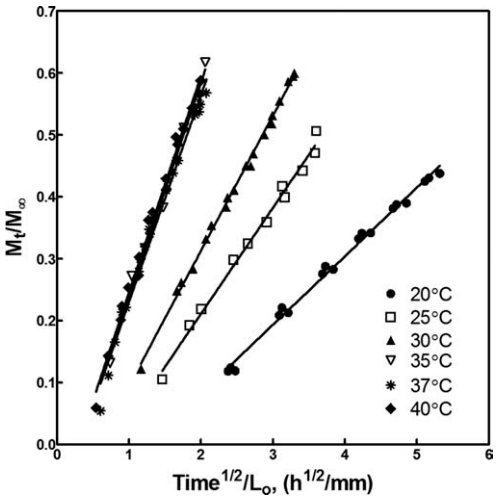

Figure 7. Effect of temperature on PMMA disks with a crosslinking density of 0.023 dried for 24 h at 10°C below T_g and swollen in methanol (linear regressions shown).

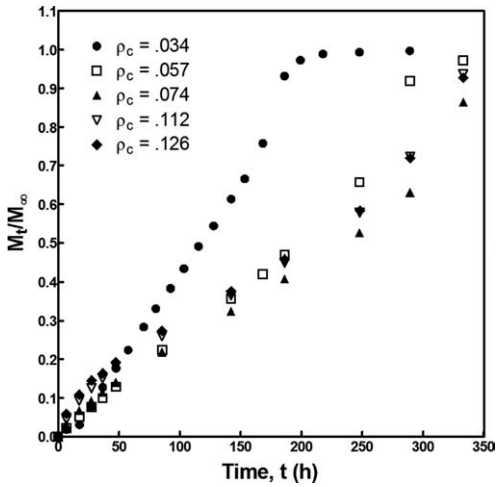

Figure 9. Effect of high crosslinking density (ρ_c) on penetrant transport for PMMA disks crosslinked with EGDMA and swollen in methanol at 25°C.

that remained. Figure 7 plots these data vs. the square root of time and shows linear regressions of the data (all regressions had an R^2 value of greater than 0.99). When these data were fit to Eq. 13, the activation energy was calculated as 24.5 kcal/mol ($R^2 = 0.96$).

This result implies that transport of methanol into glassy PMMA had the same activation energy whether the transport followed a Case II or Fickian regime for dry or plasticized samples, respectively. This similarity was at first unexpected. Indeed, the fact that Case II transport exhibited an apparent activation energy higher than those typically associated with Fickian diffusion and comparable to those reported for creep of glassy PMMA (17–30 kcal/mol) has been used occasionally as evidence to support the notion that Case II transport is a creep-deformation controlled, viscoelastic response of the polymer to an osmotic pressure (or an osmotic suction) created by the penetrant activity differential.[41] Additionally, values for the activation energy of methanol diffusion into rubbery PMMA have been measured in the infinite dilution limit as 19 kcal/mol.[42] Finally, some authors have reported activation energies for Case II transport into glassy PMMA as low as 20 kcal/mol.[43] Thus, the results of this investigation fall within the range of reported values, and much of the discrepancies in the literature are likely due to varying polymer properties and thermal histories.

Effects of crosslinking with EGDMA

One polymer property that has not been studied in sufficient detail as to its impact on penetrant transport in glassy polymers is the crosslinking density. In this investigation, PMMA cylinders were synthesized with varying molar amounts of EGDMA included in the polymerization feed. Figure 8 presents the results from samples of four crosslinking densities swollen in methanol at 30°C. For these lower degrees of crosslinking, the methanol–PMMA system displayed purely Case II transport dynamics, as was expected.

However, at crosslinking densities greater than 0.05, deviations from Case II transport were seen (Figure 9). The early portions of these profiles have also been magnified in Figure 10. As the crosslinking density was increased past $\rho_c = 0.05$

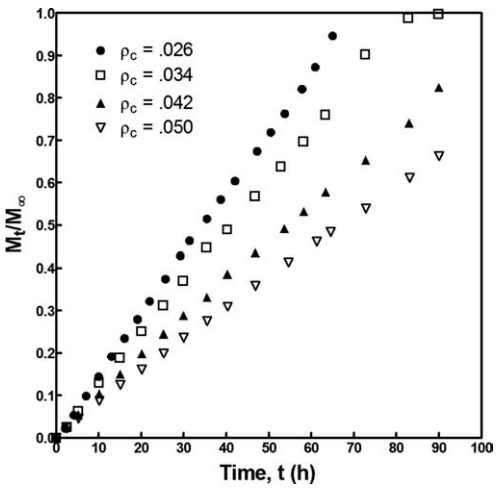

Figure 8. Effect of low crosslinking density (ρ_c) on penetrant transport for PMMA disks crosslinked with EGDMA and swollen in methanol at 30°C.

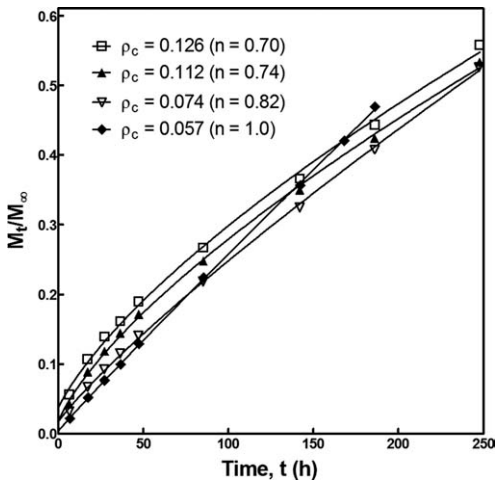

Figure 10. Power-law analysis of the effect of high crosslinking densities (ρ_c) on penetrant transport for PMMA disks crosslinked with EGDMA and swollen in methanol at 25°C.

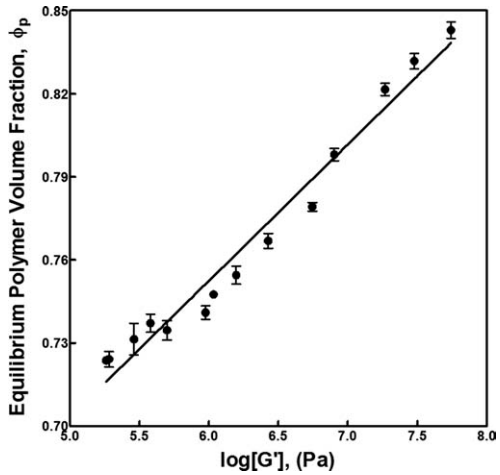

Figure 11. The variation of equilibrium polymer volume fraction, φ_p, plotted against the shear storage modulus, G', in PMMA disks crosslinked with EGDMA and swollen in methanol at 25°C.

several phenomena occurred. First, whereas before this point increasing the crosslinking density led to a reduction in the initial rate of penetrant transport, continuing to increase the crosslinking density led to faster initial rates of sorption. Second, the nature of the early transport mechanism also changed from Case II toward Fickian as ρ_c continued to increase. Returning to Figure 9, the late-time behavior can also be analyzed. Once past the initial, anomalous portion of the integral sorption curve, the rate of transport leveled out, seemingly returning to Case II dynamics in the interim region, before rapidly accelerating in rate toward the end of the sorption process.

The behavior of the samples with low crosslinking densities ($\rho_c < 0.05$) could easily be understood, as the resistance to chain relaxation was increased with increasing crosslinking and the rate of transport ought to have decreased. However, the behavior for higher crosslinking densities was far more complex. Figure 11 plots the equilibrium polymer volume fraction, φ_p, vs. the shear storage modulus, G', and sheds light on this transition in behavior. Typically, as methanol was imbibed into the polymer, at some critical concentration the T_g of the now swollen PMMA dropped below the experimental temperature. This resulted in an end-state that was a rubbery, methanol-swollen PMMA disk.

When the crosslinking density was increased, the amount of penetrant that can ultimately be sorbed by the polymer sample was decreased. At some point, the polymer could no longer absorb sufficient penetrant to go through this glass/rubber transition. For methanol sorption in PMMA, this point has been reported as a polymer volume fraction of $\sim$0.80.[40] Clearly, the deviations from Case II transport in this instance occurred only once the polymer-penetrant end-state was glassy rather than rubbery (the deviations occurred significantly in the last three points in Figure 11 and to a lesser degree in the point before the last three).

On first examination, this lent credence to the idea that a glassy polymer must have a rubbery end-state for Case II transport to occur. However, it has been shown by several previous investigators that Case II transport can occur regardless of whether or not the swollen polymer end-state is rubbery or glassy.[40,44,45] What likely occurred in this case was that the increased relaxational resistances of the polymer forced the establishment of a very significant Fickian precursor. Thus, initial sorption into the polymer was due entirely to the establishment of the precursor. Once the edge of the polymer had absorbed enough penetrant to relax and expand further, a sorption front was established and propagated inward, leading to the steady-rate portion of the integral sorption curve. This continued until the significant Fickian precursors met one another in the center of the polymer and began to overlap. Once this occurred, the dry polymer core disappeared along with the associated stresses that were necessary for the sorption front to propagate. This led to a rapid increase in the sorption of penetrant, as the polymer disk underwent structural rearrangement toward an effectively isotropically swollen end-state.

Returning to Figure 11, the equilibrium polymer volume fraction, φ_p, varied linearly with G', meaning that φ_p was dependent on the total number of effective crosslinks (chemical crosslinks and trapped entanglements). In contrast, when the Case II front velocity, V_{II}, (normalized by φ_s) was plotted vs. G' (data not shown), a change in slope after the point at which all entanglements have been entrapped (as seen in Figure 2) was observed. This indicated that the Case II front velocity depended not on the total number of effectively permanent crosslinks but on the number of effective crosslinks in the glassy state. In the glassy state, all entanglements act as crosslink points, not just the ones that are permanently entrapped.

Thus, it was more appropriate to plot the normalized Case II front velocity vs. the crosslinking density (ρ_c). The normalized velocity decreased monotonically, though at increasingly diminished rates, as the crosslinking density was increased. A nonlinear power-law model regression of this curve gave an exponent, n, of 0.52. Thus, the Case II front velocity, V_{II}, varied linearly with the square root of the crosslinking density, ρ_c (as shown in Figure 12). To the best of our knowledge, this was a novel finding of this investigation. This relationship was further confirmed for PMMA polymers crosslinked with EGDMA and swollen in methanol at 30°C (data not shown).

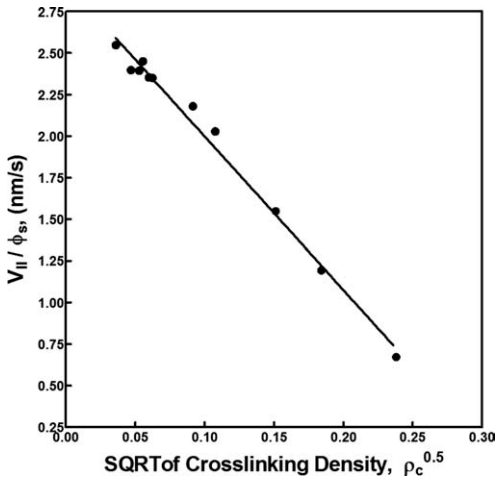

Figure 12. Normalized (by φ_s) Case II front velocity, V_{II}, vs. the square root of the crosslinking density, $\rho_c^{0.5}$, in PMMA disks crosslinked with EGDMA and swollen in methanol at 25°C.

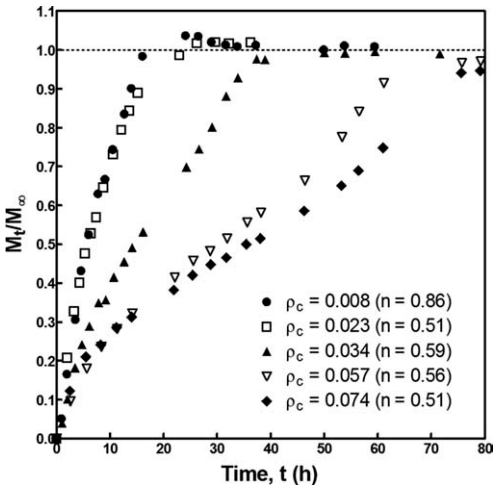

Figure 13. Effect of crosslinking density (ρ_c) on penetrant transport for PMMA disks crosslinked with EGDMA, dried/annealed for 24 h at 10°C below T_g, and swollen in methanol at 30°C.

Additionally, the effects of crosslinking with EGDMA were investigated in plasticized samples of PMMA (disks dried/annealed for 24 h at 10°C below T_g). Figure 13 displays the complete profiles of these plasticized polymers swelling in methanol at 30°C. The early time (first 60% of swelling) power-law model exponents are also shown. In a similar manner to the fully dried polymers, the integral sorption curves for crosslinking greater than $\rho_c = 0.05$ were initially Fickian, moved toward a constant rate uptake, and finally rapidly accelerated near the end of swelling. As was the case when examining the temperature dependence, plasticizing the polymer with unreacted monomer greatly reduced the relative time scales of the processes occurring and moved transport dynamics from Case II to Fickian at low crosslinking densities.

However, at higher crosslinking densities, analogous behavior to that of the fully dried polymer was seen in terms of the transport mechanism. This indicated that as the crosslinking density continued to increase, a limit was reached where the presence of a plasticizing species had a reduced effect on the relative increase of chain motion. In other words, at some point there was a sufficient quantity of crosslinks such that the crosslinks themselves became the limiting factor in chain motion. The presence of the unreacted monomer will increase the free volume present in the polymer and enhance the rate of diffusion of a penetrant into the polymer. However, with more crosslinking points per chain, a higher concentration of penetrant will be required to initiate a propagating sorption front. Thus, a more substantial Fickian precursor was formed, and once again there was an uptick in sorption rate once the precursors met in the center of the polymer and spatial rearrangement began.

Finally, an additional consequence of this two-stage/super Case II mechanism was that the polymers no longer overshot their final equilibrium penetrant concentration (as shown in Figure 12), which agreed in nature with previous data.[16,17] This demonstrated that the presence of the overshoots in these systems was initially a result of the anisotropic swelling nature of sorption in glassy polymers. In other words, the equilibrium degree of penetrant sorption was higher in the stressed polymer gel than in the final polymer end-state.

Conclusions

PMMA samples were synthesized, dried, annealed, and the integral sorption of methanol into PMMA disks was examined via gravimetric methods. The synthesis procedure used allowed for precise control over the polymer network structure, and polymerization and sample preparation procedures were optimized so as not to influence the observed transport mechanisms or rates. One of the primary findings of this investigation was the degree to which the transport process can be manipulated and altered through simple crosslinking of the polymer. It was shown that polymer systems can be taken from Fickian transport to anomalous to Case II transport and then beyond that to a two-stage/super Case II mechanism simply by increasing the number of chemical crosslinks. The ultimate scaling of the dynamics of Case II transport with network structure was shown to be straightforward; namely, the Case II front velocity was proportional to the square root of the crosslinking density ($V_{II} \propto \rho_c^{0.5}$). As a result of the interrelation of the crosslinking density, the molecular weight between crosslinks, and the polymer mesh size, this conclusion led directly to two analogous scalings: the Case II front velocity was proportional to the molecular weight between crosslinks to the -0.5 power ($V_{II} \propto M_c^{-0.5}$) and proportional to the polymer mesh size ($V_{II} \propto \xi$).

Data also showed that control over this crosslinking effect on the Case II front velocity was determined by the properties of the polymer in the glassy state. This was demonstrated clearly from data indicating that the front velocity was determined not only by the number of permanent crosslinks but also by the total number of entanglement points in the glassy state. The polymer end-state did, though, alter the transport phenomena observed at long times. When the polymer remained glassy at the equilibrium degree of sorption, the ability of the polymer to undergo major structural rearrangement from an anisotropically swelling dynamic gel to an isotropically swollen end-state was hindered, and the long-time dynamics were anomalous. Finally, similarities between the underlying controlling processes for methanol sorption into both dry and plasticized PMMA were noted. The activation energies for transport and the behavior at high crosslinking densities were found to be similar regardless of whether the mechanism was Fickian or Case II at low crosslinking densities.

Acknowledgments

A.K.E. acknowledges the National Science Foundation for a Graduate Research Fellowship and the Department of Defense for a National Defense Science and Engineering Graduate Fellowship. This research was supported by the Pratt Trust.

Literature Cited

1. Fujita H, Kishimoto A. Diffusion-controlled stress relaxation in polymers. II. Stress relaxation in swollen polymers. *J Polym Sci*. 1958;28(118):547–567.
2. Hartley GS. Diffusion and swelling of high polymers. Part III. Anisotropic swelling in oriented polymer film. *Trans Faraday Soc*. 1949;45:820–832.
3. Alfrey T, Gurnee EF, Lloyd WG. Diffusion in glassy polymers. *J Polym Sci, Part C: Polym Symp*. 1966;12:249–261.
4. Hartley GS. Diffusion and swelling of high polymers. Part I. The swelling and solution of a high polymer solid considered as a diffusion process. *Trans Faraday Soc*. 1946;42:B006–B011.
5. Crank J.*The Mathematics of Diffusion*, 2nd ed. New York, NY: Oxford University Press, 1975.

6. King G. Sorption of vapours by keratin and wool. *Trans Faraday Soc*. 1945;41:325–332.
7. Ferry JD.*Viscoelastic Properties of Polymers*, 3rd ed. New York, NY: Wiley, 1980.
8. Sinclair GW, Peppas NA. Analysis of non-Fickian transport in polymers using simplified exponential expressions. *J Membr Sci*. 1984; 17(3):329–331.
9. Hui CY, Wu KC, Lasky RC, Kramer EJ. Case-II diffusion in polymers. 1. Transient swelling. *J Appl Phys*. 1987;61(11):5129–5136.
10. Hui CY, Wu KC, Lasky RC, Kramer EJ. Case-II diffusion in polymers. 2. Steady-state front motion. *J. Appl Phys*. 1987;61(11):5137–5149.
11. Lasky RC, Kramer EJ, Hui CY. Temperature-dependence of case-II diffusion. *Polymer*. 1988;29:1131–1136.
12. Lasky RC, Kramer EJ, Hui CY. The initial-stages of case-II diffusion at low penetrant activities. *Polymer*. 1988;29(4):673–679.
13. Hassan MM, Durning CJ. Effects of polymer molecular weight and temperature on case II transport. *J Polym Sci Part B: Polym Phys*. 1999;37(22):3159–3171.
14. Kwei TK, Zupko HM. Diffusion in glassy polymers. I. *J Polym Sci, Part A-2: Polym Phys*. 1969;7(5):867–877.
15. Robert CCR, Buri PA, Peppas NA. Effect of degree of crosslinking on water transport in polymer microparticles. *J Appl Polym Sci*. 1985;30:301–306.
16. Peppas NA, Urdahl KG. Anomalous penetrant transport in glassy-polymers. 7. Overshoots in cyclohexane uptake in cross-linked polystyrene. *Polym Bull*. 1986;16(2–3):201–207.
17. Smith MJ, Peppas NA. Effect of the degree of crosslinking on penetrant transport in polystyrene. *Polymer*. 1985;26(4):569–574.
18. Otsu T, Matsumoto A. Controlled synthesis of polymers using the iniferter technique: developments in living radical polymerization. In: Abe A, Albertson AC, Cantow HJ, Dusek K, Edwards S, Hocker H, Joanny JF, Kausch HH, Kobayashi T, Lee KS, McGrath JE, Monnerie L, Stupp SI, Suter UW, Thomas EL, Wegner G, Young RJ, editors. Advances in Polymer Science, Vol. 136. New York, NY: Springer, 1998:75–137.
19. Otsu T. Iniferter concept and living radical polymerization. *J Polym Sci Part A: Polym Chem*. 2000;38(12):2121–2136.
20. Ward JH, Bashir R, Peppas NA. Micropatterning of biomedical polymer surfaces by novel UV polymerization techniques. *J Biomed Mater Res*. 2001;56(3):351–360.
21. Ward JH, Peppas NA. Kinetic gelation modeling of controlled radical polymerizations. *Macromolecules*. 2000;33(14):5137–5142.
22. Ward JH, Shahar A, Peppas NA. Kinetics of 'living' radical polymerizations of multifunctional monomers. *Polymer*. 2002;43(6):1745–1752.
23. Kazmaier PM, Moffat KA, Georges MK, Veregin RPN, Hamer GK. Free-radical polymerization for narrow-polydispersity resins—semi-empirical molecular-orbital calculations as a criterion for selecting stable free-radical reversible terminators. *Macromolecules*. 1995; 28(6):1841–1846.
24. Lambrinos P, Tardi M, Polton A, Sigwalt P. The mechanism of the polymerization of normal-butyl acrylate initiated with *N,N*-diethyl dithiocarbamate derivatives. *Eur Polym J*. 1990;26(10):1125–1135.
25. Otsu T, Matsunaga T, Kuriyama A, Yoshioka M. Living radical polymerization through the use of iniferters—controlled synthesis of polymers. *Eur Polym J*. 1989;25(7–8):643–650.
26. Manga JD, Polton A, Tardi M, Sigwalt P. Living character of the polymerization of butyl acrylate initiated by a model *N,N*-diethyldithiocarbamate. *J Macromol Sci, Part A: Pure Appl Chem*. 1995; A32:695–703.
27. Kannurpatti AR, Lu SX, Bunker GM, Bowman CN. Kinetic and mechanistic studies of iniferter photopolymerizations. *Macromolecules*. 1996;29(23):7310–7315.
28. Zaremskii MY, Olenin AV, Garina YS, Kuchanov SI, Golubev VB, Kabanov VA. Mechanism of photoinitiated radical polymerization of styrene in the presence of benzyldithiocarbamate iniferter. *Vysokomol Soedin, Ser A*. 1991;33(10):2167–2175.
29. Luo N, Metters AT, Hutchison JB, Bowman CN, Anseth KS. A methacrylated photoiniferter as a chemical basis for microlithography: micropatterning based on photografting polymerization. *Macromolecules*. 2003;36(18):6739–6745.
30. Otsu T, Yoshida M. Role of initiator-transfer agent-terminator (iniferter) in radical polymerizations—polymer design by organic disulfides as iniferters. *Makromol Chem, Rapid Commun*. 1982;3(2): 127–132.
31. Turner SR, Blevins RW. Photoinitiated block copolymer formation using dithiocarbamate free-radical chemistry. *Macromolecules*. 1990; 23(6):1856–1859.
32. Flory PJ.*Principles of Polymer Chemistry*. Ithaca, NY: Cornell University Press, 1953.
33. Mao RS, Liu Y, Huglin MB, Holmes PA. Determination of monomer reactivity ratios in the cross-linking copolymerization of methyl-methacrylate with ethylene dimethacrylate. *Macromolecules*. 1995;28(20):6739–6744.
34. Fox TG, Loshaek S. Influence of molecular weight and degree of crosslinking on the specific volume and glass temperature of polymers. *J Polym Sci*. 1955;15:371–390.
35. Ferry JD.*Viscoelastic Properties of Polymers*, 3rd ed. New York, NY: Wiley, 1980.
36. Loshaek S. Crosslinked polymers. II. Glass temperatures of copolymers of methyl methacrylate and glycol dimethacrylates. *J Polym Sci*. 1955;15:391–404.
37. Sekkar V, Narayanaswamy K, Scariah KJ, Nair PR, Sastri KS, Ang HG. Evaluation by various experimental approaches of the crosslink density of urethane networks based on hydroxyl-terminated polybutadiene. *J Appl Polym Sci*. 2007;103(5):3129–3133.
38. Brandrup J, Immergut EH, editors. *Polymer Handbook*, 3rd ed. New York, NY: Wiley, 1989.
39. Chen JK, Kuo SW, Kao HC, Chang FC. Thermal properties, specific interactions, and surface energies of PMMA terpolymers having high glass transition temperatures and low moisture absorptions. *Polymer*. 2005;46(7):2354–2364.
40. Thomas NL, Windle AH. Transport of methanol in poly(methyl methacrylate). *Polymer*. 1978;19(3):255–265.
41. Thomas NL, Windle AH. A deformation model for case-II diffusion. *Polymer*. 1980;21(6):613–619.
42. Arnould D, Laurence RL. Size effects on solvent diffusion in polymers. *Ind Eng Chem Res*. 1992;31(1):218–228.
43. Lee SB, Fu TM. Methanol transport in cross-linked poly(methyl methacrylate). *Polymer*. 1995;36(20):3975–3978.
44. Jacques CHM, Hopfenberg HB. Vapor and liquid equilibria in glassy polyblends of polystyrene and poly(2,6-dimethyl-1,4-phenylene oxide). 1. *Polym Eng Sci*. 1974;14(6):441–448.
45. Jacques CHM, Hopfenberg HB, Stannett VT.Super case II transport of organic vapors in glassy polymers. In: *Abstracts of Papers of the American Chemical Society*. 1974;51–51.

Manuscript received Aug. 5, 2011, and revision received Sept. 28, 2011.